Quantum noise limits to simultaneous quadrature amplitude and phase stabilization of solid-state lasers

E. H. Huntington,[1] C. C. Harb,[1,2] M. Heurs,[3] and T. C. Ralph[4]
[1]*School of Information Technology and Electrical Engineering, University College, The University of New South Wales, Canberra, ACT, 2600, Australia*
[2]*Australian Centre for Quantum-Atom Optics, Australian National University, Canberra, ACT 0200, Australia*
[3]*Max-Planck-Institut für Gravitationsphysik (Albert-Einstein-Institut) and Institut für Gravitationsphysik, Universität Hannover, Callinstrasse 38, D-30167 Hannover, Germany*
[4]*Department of Physics, University of Queensland, Brisbane 4072, QLD, Australia*
(Received 21 April 2006; revised manuscript received 2 August 2006; published 5 January 2007)

A quantum mechanical model is formulated to describe the coupling between pump intensity noise and laser frequency noise in a solid-state laser. The model allows us to investigate the limiting effects of closed-loop stabilization schemes that utilize this coupling. Two schemes are considered: active control of the quadrature phase noise of the laser and active control of the amplitude noise of the laser. We show that the noise of the laser in the actively stabilized quadrature is ultimately limited by the vacuum noise introduced by the feedback beamsplitter in both schemes. In the case of active control of the quadrature phase noise, the noise is also limited by the intensity noise floor of the detection scheme. We also show that some sources of noise in the passively stabilized quadrature can be suppressed and that it is possible to achieve simultaneous quadrature amplitude and phase stabilization of a solid-state laser. However, the quantum mechanically driven noise in the passively stabilized quadrature cannot be suppressed. While this poses the ultimate limit to the noise in the passively stabilized quadrature, we show that it is experimentally feasible to observe squeezing directly generated by a solid-state laser using this technique.

DOI: 10.1103/PhysRevA.75.013802 PACS number(s): 42.50.Lc, 42.55.Rz, 42.60.Mi

I. INTRODUCTION

Extremely stable lasers are required as the light sources in high precision metrology experiments such as interferometric gravitational wave detectors [1–4] and in quantum optics experiments [5]. Solid-state lasers, particularly those in a miniature monolithic architecture [6], have high intrinsic stability and are therefore the lasers of choice in these experiments. However, given that laser fluctuations approaching the quantum noise limit (QNL) would be preferred in such experiments, even miniature monolithic solid-state lasers are not sufficiently stable at all relevant frequencies [7]. Active control of either or both the intensity and frequency of the laser is commonly used to achieve the required stability.

In applications where the noise of the stabilized laser approaches the QNL, a quantum mechanical theory of both the laser and the feedback loop is required. For example, quantum mechanical theory shows that the output noise of an active stabilization system is limited by the vacuum noise introduced at the feedback beamsplitter [8,9]. More recently, a linearized quantum mechanical model of an amplitude stabilization scheme which explicitly included feedback to the pump source of the laser predicted the same result [10]. This prediction was tested experimentally in the same reference. The effect of this type of feedback loop, often referred to as a noise-eater, on the quadrature phase noise was not considered.

Recent experiments have shown that there exists a coupling between the intensity noise of the pump in a diode pumped Nd:YAG laser and the frequency noise of the laser. These experiments have shown that the coupling is strong enough to frequency lock the laser to a reference cavity by feeding back to the intensity of the pump source via the current to the pump diode lasers [11]. This technique has been dubbed current lock. Subsequent experiments have shown that the intensity noise of the laser can be reduced over the active bandwidth of the current lock feedback loop [12,13]. In other words, the quadrature amplitude noise undergoes some degree of passive stabilization as a consequence of the active phase stabilization loop.

A quantum mechanical model of the current lock technique would lead to a better understanding of the interplay between amplitude and frequency noise suppression. Furthermore, a quantum mechanical model would lead to an estimate of the ultimate achievable stability by these techniques. The purpose of this paper is to develop such a model and to determine if there are noise penalties when using these control loops.

It is common to lock the frequency of a laser to a high stability reference frequency such as a spectroscopic feature and/or a reference cavity. Figure 1(a) illustrates the laser frequency stabilization scheme where the locking signal is fed back to the optical power of the pump source using the Pound-Drever-Hall (PDH) locking system [14]. Another common stabilization technique that is applied to solid-state lasers is to suppress the intensity noise of the laser using a feedback loop. Such systems have been dubbed noise-eaters and Fig. 1(b) illustrates such an intensity noise suppression scheme.

The laser system consists of a pump diode laser, a power source to supply current and to temperature stabilize the diode laser, and a Nd:YAG laser crystal. The frequency control loop requires a fraction of the Nd:YAG laser power to be sent via a phase modulator to an optical cavity (OC) using

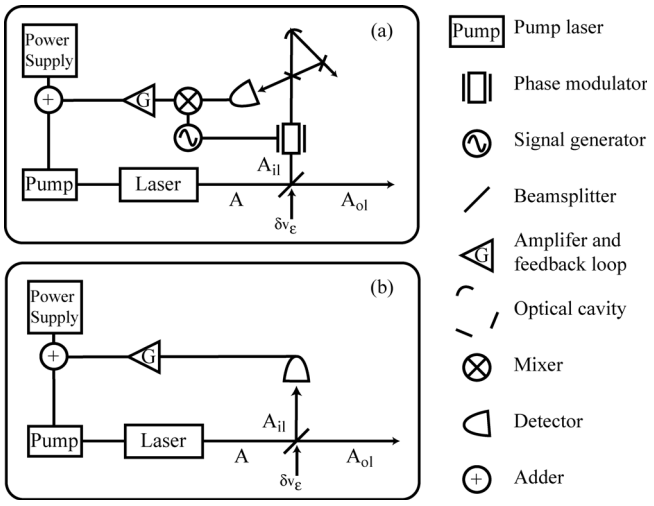

FIG. 1. (a) A schematic diagram of frequency stabilization scheme using current lock. (b) A schematic diagram of the intensity stabilization scheme (noise-eater).

a partially reflecting beamsplitter, and the signal reflected off the OC to be detected on a high speed and quantum noise limited photodetector. The photocurrent is demodulated to produce an error signal for use in the feedback loop. The intensity noise-eater, on the other hand, requires a fraction of the Nd:YAG laser power to be sent directly to a high speed and quantum noise limited photodetector, using a partially reflecting beamsplitter. The control signal in this case is the difference between the photocurrent and some precision voltage reference.

The model we will present in this paper will show that there exist two well defined regimes for the system depicted in Fig. 1. In the first regime the laser pump noise is large and hence raises the laser noise to a level well above the quantum noise limit. In the second regime the pump noise is small so the laser output noise is limited by the internal laser dynamics.

The paper is structured as follows: In Sec. II the coupling between pump intensity and laser frequency is incorporated into a linearized quantum mechanical model for a solid-state laser. The limits to the quadrature amplitude and phase noise of the laser under closed-loop frequency feedback are discussed in Sec. III. The behavior of the laser under closed-loop intensity feedback is discussed in Sec. IV and we conclude in Sec. V.

II. LASER THEORY

The basic laser model has been discussed in previous publications [7]. Here we extend the analysis to include thermally induced coupling between the intensity noise (also known as quadrature amplitude noise) of the pump source and the quadrature phase noise spectrum of the laser. Solutions for the dynamics of the laser are most conveniently found in the Heisenberg picture where we decompose travelling wave optical operators as $\hat{A}_k=\bar{A}_k+\delta\hat{A}_k(t)$, where $\bar{A}_k=\langle\hat{A}_k\rangle$, and write the operator for the internal laser mode as $\hat{a}=\bar{a}+\delta\hat{a}(t)$ with $\bar{a}=\langle\hat{a}\rangle$. Quadrature amplitude and phase fluctuation operators for an arbitrary field $\hat{A}_k$ are defined, respectively, as $\delta\hat{X}_k^+=\delta\hat{A}_k+\delta\hat{A}_k^\dagger$ and $\delta\hat{X}_k^-=i(\delta\hat{A}_k-\delta\hat{A}_k^\dagger)$.

The active atoms of the laser are modeled by a three-level system with lasing occurring between the upper two levels. Incoherent pumping occurs at a rate Γ, spontaneous emission from the upper laser level occurs at a rate γ_t and from the lower lasing level at a rate γ. The coupling of the lasing transition to the laser mode is given by K which is proportional to the stimulated emission cross section of the transition. The total cavity decay rate 2κ comprises components due to output coupling $\kappa_m=Tc/2nl$ and intracavity losses $\kappa_l=Lc/2nl$ and is given by $2\kappa=2(\kappa_m+\kappa_l)$. Here T is the transmissivity of the laser output coupler, L denotes the losses in the cavity, c is the speed of light in vacuum, l is the physical path length of the laser cavity, and n is the refractive index of the laser medium. The population of an atomic energy level k is given by J_k.

In a system such as Nd:YAG the depletion of the ground-state population is very small and so $J_1\approx 1$. Also, the population probability of the lower lasing level is very small due to its rapid decay rate (i.e., $J_2<<1$). We also make the approximation that expectation values can be factorized. Under these conditions, the steady-state solution for the internal laser mode may be found [7]:

$$\bar{a}\approx\sqrt{\frac{K\Gamma-2\kappa\gamma_t}{2\kappa K}}. \tag{1}$$

After linearization around this steady-state solution the quadrature amplitude and phase fluctuations of the output of the laser are most easily calculated and expressed as transfer functions in the Fourier domain as follows [15,16]:

$$\delta X^+(\omega)=F_v^+\delta X_v^+ + F_p^+\delta X_{p1}^+ + F_{\rm sp}^+\delta X_{\rm sp}^+ + F_{\rm dip}^+\delta X_{\rm dip}^- + F_l^+\delta X_l^+, \tag{2}$$

$$\delta X^-(\omega)=F_v^-\delta X_v^- + F_{p1}^-\delta X_{p1}^+ + F_{p2}^-\delta X_{p2}^+ + F_p^-\delta X_{ps} + F_{\rm dip}^-\delta X_{\rm dip}^- + F_l^-\delta X_l^- + F_{\rm cav}\delta X_{\rm cav}, \tag{3}$$

$$F_v^+=\frac{2\kappa_m(\gamma_l+i\omega)}{(\omega_r^2-\omega^2)+i\omega\gamma_l}-1,$$

$$F_p^+=\frac{\sqrt{2\kappa_m\Gamma}K\bar{a}}{(\omega_r^2-\omega^2)+i\omega\gamma_l},$$

$$F_{\rm sp}^+=\frac{\sqrt{4\kappa_m\gamma_t\kappa K}\bar{a}}{(\omega_r^2-\omega^2)+i\omega\gamma_l},$$

$$F_{\rm dip}^+=\frac{\sqrt{4\kappa_m\kappa}[(\gamma_t+\Gamma)+i\omega]}{(\omega_r^2-\omega^2)+i\omega\gamma_l},$$

$$F_l^+=\frac{\sqrt{4\kappa_m\kappa_l}(\gamma_l+i\omega)}{(\omega_r^2-\omega^2)+i\omega\gamma_l},$$

$$F_v^- = \frac{2\kappa_m}{i\omega} - 1, \quad F_{\rm dip}^- = \frac{\sqrt{4\kappa_m\kappa}}{i\omega},$$

$$F_l^- = \frac{4\sqrt{\kappa_m\kappa_l}}{i\omega}, \quad F_{\rm cav} = -2\omega_{ax}\frac{\bar{A}}{i\omega},$$

$$\omega_r = \sqrt{2\kappa K\bar{a}^2}, \quad \gamma_l = K\bar{a}^2 + \gamma_t + \Gamma, \tag{4}$$

where the absence of hats on the fluctuation operators signifies that we have made the transformation to the Fourier domain. The steady-state photon flux emerging from the laser is $|\bar{A}|^2 = 2\kappa_m N_T |\bar{a}|^2$ and N_T is the number of active atoms contributing to the laser mode. Other parameters are ω_r, the resonant relaxation oscillation (RRO) frequency, and $\omega_{ax} = qc/nl$ the resonant frequency of the laser cavity (for q an integer).

The input noise operators are noise from the vacuum field entering at the output coupler, $\delta X_v^{\pm}(\omega)$, dipole fluctuation noise, $\delta X_{\rm dip}^-(\omega)$, noise introduced from intracavity losses, $\delta X_l^{\pm}(\omega)$, noise from spontaneous emission out of the upper laser level, $\delta X_{\rm sp}^+$, and noise introduced by fluctuations of the length of the cavity, $\delta X_{\rm cav} = \frac{\langle \delta nl \rangle}{nl}$, where $\langle \delta nl \rangle$ are the fluctuations in the optical path length of the cavity and nl is the average optical path length. The noise of the pump source δX_p^+ couples to the amplitude quadrature according to the pumping efficiency η_i such that $\delta X_{p1}^+ = \sqrt{\eta_i}\delta X_p^+ + \sqrt{1-\eta_i}\delta X_{vp}^+$, where δX_{vp}^+ is a vacuum operator. We also have $\delta X_{p2}^+ = \sqrt{1-\eta_i}\delta X_p^+ - \sqrt{\eta_i}\delta X_{vp}^+$.

Most of these transfer functions have been discussed in previous publications (see, for example, [15] for plots of transfer functions to intensity noise and [16] for transfer functions to phase noise). Here we identify the new transfer functions F_{p1}^-, F_{p2}^-, and F_p^- representing the coupling of intensity noise of the pump source and other spontaneous noise sources to the phase noise of the laser due to the dissipation of excess pump energy in the medium.

Excess pump energy is released by the decay of the lower lasing level (level 2) as phonons can couple to the medium. In contrast we assume spontaneous photons emitted as a result of upper lasing level decay do not couple to the medium. Excess pump energy is released both by active (i.e., lasing) atoms and by inactive atoms. In both cases the energy released is proportional to $\gamma\langle \hat{J}_2 \rangle$. In turn the quantum fluctuations in this energy are proportional to $\gamma\delta\hat{J}_2$, where $\delta\hat{J}_2 = \langle \hat{J}_2 \rangle - \hat{J}_2$. From the fluctuation equations given in [7] we derive the following transfer function describing the contribution of pump fluctuations to energy fluctuations arising from the decay of active atoms:

$$E_1 = \frac{K\eta_i 2\kappa\bar{a} - i\omega(\bar{a}^2K + \gamma_t)}{E_d},$$

$$E_d = (K\eta_i 2\kappa\bar{a} - i\omega K\bar{a}^2)(\gamma + 2i\omega) - i\omega(\gamma_t + i\omega)(\gamma + i\omega) \tag{5}$$

Additional spontaneous noise terms also coupled to the phase noise through this mechanism are given by

$$X_{ps1} = \gamma\sqrt{\frac{\lambda_p}{hcP_p}}\frac{K\eta_i 2\kappa\bar{a} - i\omega(\bar{a}^2K + \gamma_t)}{E_d}\sqrt{\eta_i\Gamma}\,\delta X_2^+,$$

$$X_{ps2} = \gamma\sqrt{\frac{\lambda_p}{hcP_p}}\frac{-i\omega\eta_i 2\kappa(\sqrt{\kappa_l}\delta X_l^+ + \sqrt{\kappa_m}\delta X_v^+)}{E_d},$$

$$X_{ps3} = \frac{i\omega\gamma(\eta_i 2\kappa - \bar{a}i\omega)}{E_d}\sqrt{\frac{\lambda_p K[\eta_i\Gamma\gamma_t - \gamma(2\kappa\bar{a} - \eta_i\Gamma)]}{hcP_p\gamma\gamma_t}}\delta X_{\rm dip}^-,$$

$$X_{ps4} = -\gamma\sqrt{\frac{\lambda_p}{hcP_p}}\frac{\omega^2}{E_d}\sqrt{\eta_i\Gamma - 2\kappa\bar{a}}\,\delta X_{\rm sp}^+, \tag{6}$$

where δX_2^+ is noise due to spontaneous emission out of the lower laser level. The energy dissipated by the inactive atoms, mechanism (ii), also gives rise to a pump noise transfer function given by

$$E_2 = \frac{\gamma_t}{E_{\rm di}}, \quad E_{\rm di} = (\gamma_t + i\omega)(\gamma + i\omega), \tag{7}$$

and spontaneous noise terms

$$X_{ps5} = \sqrt{\frac{\lambda_p}{hcP_p}}\frac{\gamma\gamma_t}{E_{\rm di}}\sqrt{(1-\eta_i)\Gamma}\,\delta X_2^+,$$

$$X_{ps6} = \sqrt{\frac{\lambda_p}{hcP_p}}\frac{i\omega\gamma}{E_{\rm di}}\sqrt{(1-\eta_i)\Gamma}\,\delta X_{\rm sp}^+. \tag{8}$$

The coupling of the energy fluctuations to the phase noise of the laser is modeled as thermally induced changes in the optical path length of the laser cavity which then couple to the quadrature phase fluctuations of the laser via $F_{\rm cav}$. Putting everything together the new transfer functions are

$$F_{p1}^- = \gamma\sqrt{\eta_i}E_1F_p^-,$$

$$F_{p2}^- = \gamma\sqrt{(1-\eta_i)}E_2F_p^-,$$

$$F_p^- = F_{\rm cav}[\alpha_n + (n-1)(1+\sigma)\alpha + n^3\alpha C_{t,\phi}]\chi_T F_T/n,$$

$$\chi_T = \frac{\zeta_T}{kl}\sqrt{P_p\frac{hc}{\lambda_p}\left(1 - \frac{\lambda_p}{\lambda_l}\right)}, \quad F_T \approx \frac{1}{1 + i\omega\tau_T},$$

$$\tau_T \approx \rho C r_0^2/k, \quad \delta X_{ps} = \Sigma_{i=1,6}X_{psi}. \tag{9}$$

At low frequencies $E_1 = E_2 = 1/\gamma$ and thus the expression for the quadrature phase fluctuations simplifies to

$$\delta X^- = F_v^-\delta X_v^- + F_p^-\delta X_p^+ + F_{\rm dip}^-\delta X_{\rm dip}^- + F_l^-\delta X_l^- + F_{\rm cav}\delta X_{\rm cav}, \tag{10}$$

where F_p^- is as defined in Eq. (9) and the contribution of the spontaneous emission noise term δX_{ps} is wrapped up in the

TABLE I. Approximate noise limits of the free-running laser at each relevant frequency region. Here, $V_{\mathrm{STL}}^{-}=8\kappa\kappa_m/\omega^2$ represents the quantum mechanically driven quadrature phase noise at low frequencies, $V_{N1}\approx(2\kappa\gamma_t/\omega_r^2)(1+2\kappa\gamma_t\Gamma^2/K^2\omega_r^2)$ represents the magnitude of the quantum mechanically driven intensity noise at low frequencies, and $V_{N2}\approx 2\kappa(4\kappa+\gamma_t)/\gamma_l^2$ represents the magnitude of the relaxation oscillation when driven by the quantum mechanical noise sources. We have assumed that the losses are negligible in making these approximations.

Phase noise		Amplitude noise	
Frequency range	Noise limit	Frequency range	Noise limit
$\omega\ll 2\pi f_T$	$V^{-}\approx V_{\mathrm{STL}}^{-}+\lvert F_p^{-}\rvert^2V_p^{+}+\lvert F_{\mathrm{cav}}\rvert^2V_{\mathrm{cav}}$	$\omega\ll\omega_r$	$V^{+}\approx V_{N1}+V_p^{+}K\Gamma/\omega_r^2$
$2\pi f_T<\omega<\kappa$	$V^{-}\approx V_{\mathrm{STL}}^{-}+\lvert F_{\mathrm{cav}}\rvert^2V_{\mathrm{cav}}$	$\omega\approx\omega_r$	$V^{+}\approx V_{N2}+V_p^{+}K\Gamma/\gamma_l^2$
$\omega\gg\kappa$	$V^{-}\approx$ QNL	$\omega\gg\omega_r$	$V^{+}\approx$ QNL

cavity length fluctuation term δX_{cav}. Also, ρ is the density of the laser material, C is the specific heat, r_0 is the radius of the pump spot, k is the thermal conductivity, $\alpha_n=(1/n)dn/dT$ characterizes the rate of change of refractive index with temperature, $\alpha=(1/l)dl/dT$ is the thermal expansion coefficient, σ is Poisson's ratio, and $C_{t,\phi}$ is the photoelastic coefficient [17–19]. Also, P_p is the average power of the pump laser, λ_p is the wavelength of the pump laser, λ_l is the wavelength of the laser emission, and h is Planck's constant.

Physically, thermally induced changes in the optical path length comprise changes in the refractive index with temperature, changes in the physical path length with temperature, and changes in the refractive index due to the stress-optic effect. These are represented, respectively, in the square brackets in Eq. (9). Conversion of energy released by the atoms into change of temperature in the laser crystal is represented by χ_T in Eq. (9), see, for example, [19,20]. The absolute magnitude of the conversion of pump power to temperature change in the crystal depends on the details of the pumping, cooling, and crystal geometries [19]. These details are absorbed into the scaling constant ζ_T. In an end-pumped, edge-cooled geometry for Nd:YAG with an approximately uniform intensity distribution for the pump, the scaling constant would lie in the range 1–100. Assuming a uniform intensity distribution in the case of a miniature monolithic Nd:YAG laser pumped by a single-mode laser is a gross approximation. Given that ζ_T is so widely varying (it depends on pump spot size compared to the crystal cross section among other things), errors in this approximation can be absorbed by ζ_T. Note that ζ_T will not be unity for a perfect Gaussian pump spot.

The term F_T represents the thermal low-pass filter of the laser crystal for a thermal time constant of τ_T. Previous works investigating photothermally induced noise in empty cavities have shown that the transfer function is rather more complex than a simple low-pass filter [21,22]. However, the simplified transfer function will be an adequate approximation for our purposes.

The variances of the fluctuations in the quadrature amplitude and phase (called quadrature amplitude and phase noise for brevity) of a field relative to the QNL are

$$V^{\pm}=\lvert\delta X^{\pm}\rvert^2=\sum_k\lvert F_k\rvert^2V_k, \tag{11}$$

where $V=1$ implies noise at the QNL. These quantities are related to the relative intensity noise ($\mathcal{N}$) (measured in units of 1/Hz) and frequency noise of the field (measured in $\mathrm{Hz}^2/\mathrm{Hz}$) by:

$$\mathcal{N}=\frac{\lvert\delta P\rvert^2}{P^2}=\frac{V^{+}}{\bar{A}^2}, \tag{12}$$

$$V_\Omega=\lvert\delta\Omega\rvert^2=\left\lvert\frac{\omega\langle\delta X^{-}\rangle}{2\bar{A}}\right\rvert^2=\frac{\omega^2V^{-}}{4\bar{A}^2}, \tag{13}$$

where $P=\bar{A}^2hc/\lambda_l$ is the average output power of the laser, δP represents the spectral density of the power fluctuations, the frequency fluctuation spectral density (in $\mathrm{Hz}/\sqrt{\mathrm{Hz}}$) is $\lvert\delta\Omega\rvert=\omega\lvert\delta\phi\rvert$, and the quadrature phase fluctuations are related to phase fluctuations via $\lvert\delta\phi\rvert=\langle\delta X^{-}\rangle/2\bar{A}$ [16,25].

The quadrature amplitude and phase noise spectra of the laser have been discussed in detail in previous publications [7,15,16]. It will suffice here to say that the laser noise in both quadratures is the linear combination of several quantum mechanically driven noise contributions and two technical noise contributions. The two technical sources of noise are the intensity noise of the pump, which appears on both quadratures, and the optical path length fluctuations of the laser cavity, which only appears on the phase quadrature. Both the quadrature amplitude and phase noise of the laser fall into three main frequency regions. Table I summarizes the quadrature amplitude and phase noise of the laser in each of these frequency regions. The output noise has been expressed in the form of a noise floor with additive technical noise because the technical sources of noise can, at least in principle, be suppressed. When this occurs, the contributions from the quantum mechanical noise sources dominate and this noise floor represents the lowest possible output noise of the free-running laser.

Figure 2 shows the quadrature amplitude and phase noise of the laser when the intensity noise of the pump is set to the QNL and also when the intensity noise of the pump is set to an experimentally realistic value of 60 dB above the QNL. The parameters are taken directly from experimental systems [13,16]. To illustrate the coupling between pump intensity noise and laser phase noise, we have set $V_{\mathrm{cav}}\approx 0$. The Schawlow-Townes limit (STL) is normally defined in terms of frequency noise. However, Eq. (13) allows us to convert the STL into a limit in terms of quadrature phase noise such

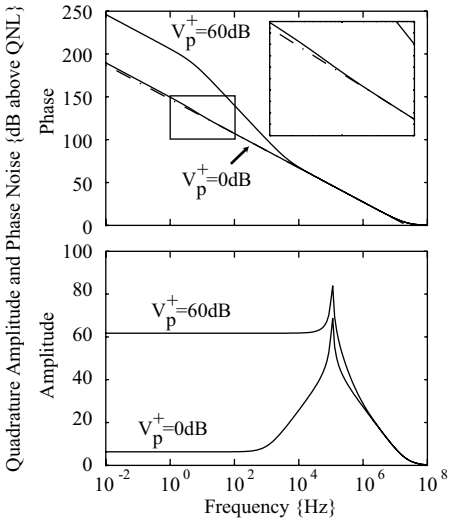

FIG. 2. Plots of the quadrature amplitude and phase noise of the laser when $V_p^+=0$ dB and when $V_p^+=60$ dB. The laser parameters used to generate these traces are $P_p=70$ mW, $\eta_p=0.552$ (pump quantum efficiency), $\lambda_p=0.813$ μm [13], $\lambda_l=1.064$ μm, $\kappa_m=4.28\times10^7$ s^{-1}, $\kappa_l=1.74\times10^7$ s^{-1}, $l=26$ mm, and $\tau_T=0.032$ s. The Nd:YAG parameters are: $n=1.82$, $\gamma_t=4.3\times10^3$ s^{-1}, $K=6.6\times10^{11}$ s^{-1}, $\zeta_T=1$, $\rho=4.55\times10^3$ kg m^{-1}, $\sigma=0.25$, $\alpha=7.2\times10^{-6}$ K^{-1}, $\alpha_n=7.3\times10^{-6}$ K^{-1}, $C=100$ JK^{-1} m^{-1}, and $C_{t,\phi}=-0.0025$ $V_{\rm cav}=0$.

that $V_{\rm STL}^-=8\kappa\kappa_m/\omega^2$ [16]—this is shown as the dash-dotted line in Fig. 2 for reference. The inset shows an expanded view of the quadrature phase noise in the region indicated to more clearly illustrate the relationship between $V_{\rm STL}$ and the quadrature phase noise for a QNL pump.

III. LASER NOISE UNDER FREQUENCY STABILIZATION

Figure 1 shows that the output of the laser is split into two beams, $\hat{A}_{\rm il}$ the in-loop field and $\hat{A}_{\rm ol}$ the out-of-loop field. A vacuum field $\delta\hat{v}_\epsilon$ is introduced at the beamsplitter such that

$$\hat{A}_{\rm il}=i\sqrt{1-\epsilon}\hat{A}+\sqrt{\epsilon}\delta\hat{v}_\epsilon,\quad \hat{A}_{\rm ol}=\sqrt{\epsilon}\hat{A}+i\sqrt{1-\epsilon}\delta\hat{v}_\epsilon, \quad (14)$$

where ϵ represents the power transmission of the beamsplitter and we have used the symmetric beamsplitter convention [23]. For frequency stabilization the in-loop field is phase modulated at ω_m with modulation index β and sent to a reference cavity with decay rate κ_c. The PDH error signal is obtained by detection of the field reflected off the reference cavity and subsequent filtering and demodulation of the detected signal (see [24–27] and the references therein for more details). We shall assume for simplicity that the cavity is already resonant with the laser frequency at dc, acoustically stabilized, lossless, and impedance matched.

The PDH error signal may be written as $v_{\rm fb}=\bar{v}_{\rm fb}+\delta v_{\rm fb}$ representing the dc and ac components of the error signal, respectively. In the Fourier domain $\delta v_{\rm fb}$ is

$$\delta v_{\rm fb}=-G\bar{A}(1-\epsilon)\left\{\beta\left(\frac{\omega}{\kappa_c+\omega}\right)\left[\delta X_A^-+\sqrt{\frac{\epsilon}{1-\epsilon}}\delta X_{v_\epsilon}^+\right]-\left(\frac{\beta}{2}\right)^2\sqrt{2}\left[\delta X_A^+(\omega+\omega_m)-\sqrt{\frac{\epsilon}{1-\epsilon}}\delta X_{v_\epsilon}^-(\omega+\omega_m)\right]\right., \quad (15)$$

where $G(\omega)$ is the electronic transfer function of the system including the gain and filtering of the electronics, the responsivity of the photodetector, and the demodulation efficiency of the mixer. We have assumed perfect quantum efficiency for the photodetector. Equation (15) is consistent with previous investigations of the measurement of laser phase fluctuations using the PDH technique [24] except that the quantum optical model explicitly shows the vacuum noise introduced at the beamsplitter.

Under closed loop feedback, the pump noise becomes $\delta X_p^+(\omega)\to\delta X_p^+(\omega)+\delta v_{\rm fb}(\omega)$. The out-of-loop quadrature amplitude and phase fluctations are given in Eqs. (16) and (17):

$$\begin{aligned}\delta X_{\rm ol}^+=&\sqrt{\epsilon}(F_v^+\delta X_v^++F_{\rm sp}^+\delta X_{\rm sp}^++F_l^+\delta X_l^+)+\sqrt{1-\epsilon}\delta X_{v_\epsilon}^-\\&+\sqrt{\epsilon}\delta X_p^+\frac{F_p^+}{1+\gamma_F}+\sqrt{\epsilon}\delta X_{\rm dip}^+\left[F_{\rm dip}^+-\frac{F_p^+\gamma_F}{1+\gamma_F}\frac{F_{\rm dip}^-}{F_p^-}\right]\\&-\sqrt{\epsilon}\frac{F_p^+}{F_p^-}\frac{\gamma_F}{1+\gamma_F}(F_v^-\delta X_v^-+F_l^-\delta X_l^-+F_{\rm cav}\delta X_{\rm cav})\\&-\frac{\epsilon}{\sqrt{1-\epsilon}}\frac{F_p^+}{F_p^-}\frac{\gamma_F}{1+\gamma_F}\delta X_{v_\epsilon}^+-\sqrt{\epsilon}\frac{F_p^+}{F_p^-}\frac{\beta}{\sqrt{8}}\frac{1}{\left(\frac{\omega}{\kappa_c+i\omega}\right)}\frac{\gamma_F}{1+\gamma_F}\\&\times\left[\delta X_A^+(\omega+\omega_m)-\sqrt{\frac{\epsilon}{1-\epsilon}}\delta X_{v_\epsilon}^-(\omega+\omega_m)\right],\end{aligned} \quad (16)$$

$$\begin{aligned}\delta X_{\rm ol}^-=&\frac{\sqrt{\epsilon}}{1+\gamma_F}(F_v^-\delta X_v^-+F_{\rm dip}^-\delta X_{\rm dip}^-+F_l^-\delta X_l^-+F_p^-\delta X_p^+\\&+F_{\rm cav}\delta X_{\rm cav})-\frac{\sqrt{1-\epsilon}\delta X_{v_\epsilon}^+[1+\gamma_F/(1-\epsilon)]}{1+\gamma_F}\\&-\sqrt{\epsilon}\frac{\beta}{\sqrt{8}}\frac{1}{\left(\frac{\omega}{\kappa_c+i\omega}\right)}\frac{\gamma_F}{1+\gamma_F}\left[\delta X_A^+(\omega+\omega_m)\right.\\&\left.-\sqrt{\frac{\epsilon}{1-\epsilon}}\delta X_{v_\epsilon}^-(\omega+\omega_m)\right],\end{aligned} \quad (17)$$

$$\gamma_F=F_p^-G(\omega)\beta\bar{A}\left(\frac{\omega}{\kappa_c+i\omega}\right)(1-\epsilon), \quad (18)$$

where γ_F is a measure of the overall gain in the feedback loop.

It is relatively straightforward to write down the output variances of the feedback loop from Eqs. (11), (16), and (17). However, the resulting equations are bulky and the limiting behavior of the system is more easily discussed by considering the output variances in the high gain limit, i.e., $\gamma_F\gg1$,

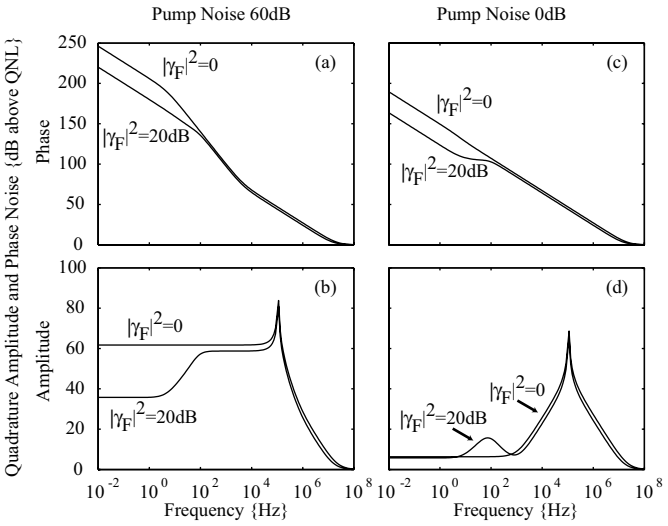

FIG. 3. Plots of the quadrature amplitude and phase noise of the laser when the current lock stabilization loop is active and inactive. The parameters used to generate these traces are the same as for Fig. 2. We also set $\beta=0.5$, $|\gamma_F|^2=20$ dB, and $\epsilon=0.5$.

and in the no gain limit, i.e., $\gamma_F \ll 1$. Physically these would normally correspond to the variances inside and outside the bandwidth of the feedback loop, respectively. The out-of-loop variances in the high and no gain limits are

$$V^+_{\mathrm{HGL}}(\omega) \approx \epsilon\left\{\left|\frac{F^+_p}{\gamma_F}\right|^2 V^+_p + V^+_{\mathrm{AO}} + \left|F^+_{\mathrm{dip}} - F^+_p\frac{F^-_{\mathrm{dip}}}{F^-_p}\right|^2 + \left|\frac{F^+_p}{F^-_p}\right|^2\left[V^-_{\mathrm{PO}} + \frac{\epsilon}{1-\epsilon} + \frac{\beta^2(\kappa_c^2+\omega^2)}{8(1-\epsilon)\omega^2}\right]\right\} + (1-\epsilon), \tag{19}$$

$$V^-_{\mathrm{HGL}}(\omega) \approx \frac{\epsilon}{|\gamma_F|^2}V^-(\omega) + \frac{1}{1-\epsilon} + \frac{\epsilon\beta^2(\kappa_c^2+\omega^2)}{8(1-\epsilon)\omega^2}, \tag{20}$$

$$V^\pm_{\mathrm{NGL}}(\omega) \approx \epsilon V^\pm + (1-\epsilon), \tag{21}$$

where V^+ and V^- are the output amplitude and phase variances, respectively, of the free-running laser as calculated using Eq. (11) and the free-running transfer functions, $V^+_{\mathrm{AO}} = V^+ - |F^+_p|^2 V^+_p - |F_{\mathrm{dip}}|^+ V^-_{\mathrm{dip}}$ and $V^-_{\mathrm{PO}} = V^- - |F^-_p|^2 V^+_p - |F^-_{\mathrm{dip}}|^2 V^-_{\mathrm{dip}}$ are the output variances of the free-running laser due to noise sources only appearing in the amplitude and phase quadratures, respectively. We have also set $V^+(\omega_m)=1$.

Figure 3 shows the quadrature amplitude and phase noise when the laser is free-running and when the frequency stabilization loop is operational for experimental parameters typical of a miniature monolithic laser. For the feedback loop, we have chosen a level of feedback gain to give an experimentally realistic $|\gamma_F|^2 \approx 20$ dB. For simplicity, we have assumed that the transfer function of the electronics is a single-pole low-pass filter with a 50 Hz corner frequency. In practice, it is more likely that the feedback controller would have a band-limited proportional-integral or proportional-integral-differential architecture.

As required, the feedback loop suppresses the original quadrature phase noise of the laser by the overall loop gain, $|\gamma_F|^2$. This noise is further diminished by virtue of the attenuation of the beamsplitter. This effect is observed in the top row of Fig. 3 where the phase noise of the laser is reduced by the loop gain $|\gamma_F|^2=20$ dB over the frequency range 0–5 Hz. Above 5 Hz, the thermal low-pass filter of the laser crystal reduces the overall loop gain as $1/f^2$ and unity gain is reached at 40 Hz. This is why the noise suppression is observed to decrease from 20 to 0 dB in the frequency range 5–40 Hz in the top row of Fig. 3. The decrease in loop gain in this scenario is due entirely to the thermal low-pass filter of the laser crystal and hence is a fundamental feature of current lock rather than an artifact of the choice of electronic transfer function.

The quadrature phase noise of frequency stabilized laser systems may drop below the STL given sufficient loop gain—for example, as in Fig. 3(c). As a guide to the eye, the curve labeled $|\gamma_F|^2=0$ in this panel approximately follows the STL for $f<1$ MHz. Although not observed in Fig. 3 because the loop gain is inadequate, the fundamental lower limit to the quadrature phase noise in this scenario is set by the vacuum noise introduced at the feedback beamsplitter and by the intensity noise floor of the PDH scheme [8,9].

Central to the physics of simultaneous stabilization of amplitude and phase quadrature noise is that the technique of feeding back to the intensity of the pump source will imprint the feedback signal onto both quadratures of the laser. Thus, in the high gain limit the current lock feedback loop acts on the amplitude as well as the phase quadrature—albeit in a less straightforward manner.

Noise common to both quadratures, such as V^+_p, can be suppressed on the amplitude quadrature. This is an extremely valuable effect from an experimental perspective as the intensity noise of the pump tends to dominate other sources of noise in current experiments. Figure 3(b) shows the intensity noise of the laser under these conditions. This result is consistent with experimental observations [12].

However, there are two other effects which limit the ultimate stability that can be achieved in the amplitude quadrature. First, the feedback signal contains no information about noise that appears only on the amplitude quadrature. Consequently, there is no suppression of this noise beyond the attenuation afforded by the beamsplitter. The second issue is that noise normally only appearing on the phase quadrature is amplified and imprinted onto the amplitude quadrature. As the former process tends to reduce intensity noise and the latter tends to increase intensity noise, the eventual intensity noise of the laser in the high gain limit depends strongly on the balance of these two competing effects.

The delicate balance between intensity noise suppression and enhancement is illustrated Fig. 3(d). At frequencies where the loop gain is greatest (i.e., $0<f<5$ Hz), these competing effects result in a slight decrease in intensity noise compared to the unstabilized laser. In the range of frequencies where the loop gain decreases due to the thermal low-pass filter (i.e., 5–40 Hz), the balance of these competing effects is shifted to the point where the intensity noise is actually greater than that of the free-running laser. Effectively, the pump noise suppression decreases while the addi-

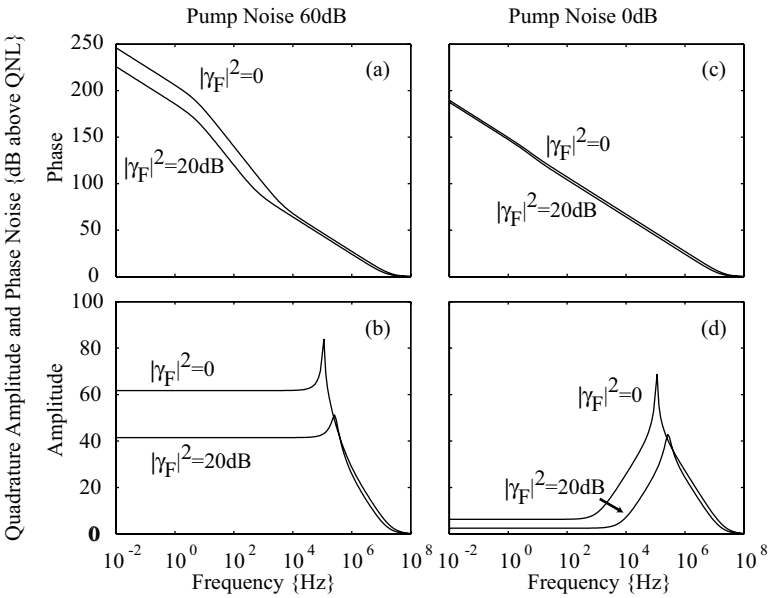

FIG. 4. Plots of the quadrature amplitude and phase noise of the laser when the noise-eater loop is active and inactive. The parameters used to generate these traces are the same as for Fig. 2. We also set $|\gamma_F|^2$=20 dB and ϵ=0.5.

tion of quadrature phase noise increases and so an increase in intensity noise results.

One somewhat negative conclusion that we can draw from the preceding discussion is that current lock cannot be used to suppress the RRO. The RRO is driven by numerous noise sources and it cannot be eliminated by suppressing the intensity noise of the pump source (see [15] and the second row of the final column in Table I). At best, current lock would suppress only that component of the RRO arising from the pump intensity noise.

A more positive outcome is that it may be possible to use this technique to generate squeezing directly from the solid-state laser. Previous work has shown that a free-running laser pumped sufficiently far above threshold can transfer the intensity noise of the pump to the output of the laser at low frequencies with minimal excess noise on the output (see [7,15] and the first row of the final column in Table I). This observation has, in the past, lead to the proposal to generate low frequency squeezing directly from a solid-state laser by pumping it well above threshold with a squeezed diode laser. The model presented here suggests that current lock allows us to arbitrarily suppress the apparent intensity noise of the pump source and hence generate amplitude squeezing directly from the laser at low frequencies. This new approach appears much more experimentally feasible than the previous proposal. For example, with η_p=0.9, V_p^+=30 dB, and all other parameters as used in Fig. 2, we find that $V_{\rm ol}^+ \approx -3$ dB at low frequencies.

Above the unity gain frequency of 40 Hz the quadrature phase and intensity noise spectra are essentially in the no gain limit. Figures 3(a)–3(d) as well as Eq. (21) show that both the amplitude and phase quadrature noise in the no gain limit are simply the variances expected from attenuation through a beamsplitter of transmittivity ϵ.

IV. LASER NOISE UNDER INTENSITY STABILIZATION

As with the frequency feedback system, the laser output is split into the in- and out-of-loop fields as given in Eq. (14). Direct detection of the in-loop beam results in the feedback signal

$$\delta v_{\rm fb} = -G(\omega)\sqrt{1-\epsilon}\bar{A}(\sqrt{1-\epsilon}\delta X_A^+ - \sqrt{\epsilon}\delta X_{v_\epsilon}^-), \qquad (22)$$

where $G(\omega)$ is the electronic gain of the system including the gain and filtering of the electronics as well as the responsivity of the photodetector. We explicitly assume ac-coupled feedback and again have assumed perfect detection efficiency. The pump amplitude fluctuations become $\delta X_p^+(\omega) \rightarrow \delta X_p^+(\omega) + \delta v_{\rm fb}(\omega)$. The variances of the out-of-loop quadrature amplitude and phase fluctations in the high gain limit are given in Eqs. (23) and (24):

$$V_{\rm HGL}^+(\omega) \approx \frac{\epsilon}{|\gamma_F|^2}V^+ + \frac{1}{1-\epsilon}, \qquad (23)$$

$$V_{\rm HGL}^-(\omega) \approx \epsilon\left\{\left|\frac{F_p^-}{\gamma_F}\right|^2 V_p^+ + V_{\rm PO} + \left|F_{\rm dip}^- - F_{\rm dip}^+\frac{F_p^-}{F_p^+}\right|^2 + \left|\frac{F_p^-}{F_p^+}\right|^2\left[V_{\rm AO}^+ + \frac{\epsilon}{1-\epsilon}\right]\right\} + (1-\epsilon), \qquad (24)$$

$$\gamma_F = F_p^+ G(\omega)\bar{A}(1-\epsilon). \qquad (25)$$

The variances of the output of the noise-eater in the no gain limit are given by Eq. (21). Figure 4 shows the quadrature amplitude and phase noise when the laser is free-running and when the frequency stabilization loop is operational. For simplicity we have assumed that the transfer function of the electronics is a single-pole low-pass filter with a 1 MHz corner frequency. In practice, it is more likely that the feedback controller would have an ac-coupled, band-limited proportional-differential architecture. The unity gain frequency of the feedback loop is approximately 300 kHz.

Direct comparison of Eqs. (23) and (24) to the equivalent equations for the current lock system reveals that the behavior of the laser under intensity stabilization is essentially the

converse of the laser under quadrature phase (or equivalently frequency) stabilization. Thus we conclude that an intensity noise-eater can be used to suppress that part of the quadrature phase noise of a laser arising from the intensity noise of the pump. This has practical consequences in that an intensity noise-eater could be used to suppress the quadrature phase noise of a laser to levels at or near the STL in situations where the cavity length fluctuations of the laser are relatively small (see [16] and the top row of the first column of Table I). Unlike a dedicated frequency stabilization loop, however, an intensity noise-eater could not suppress the phase noise of a laser below the STL and intensity noise-eaters are usually ac-coupled thereby rendering them ineffective as stand-alone frequency locking systems.

V. CONCLUSION

We have extended a previously published linearized quantum mechanical theory of solid-state lasers [7] to include the coupling between the quadrature phase noise of a laser and the amplitude noise of its pump. The coupling is mediated by thermally induced fluctuations in the optical path length of the laser crystal. We have applied the extended model to an investigation of the limits to simultaneous quadrature amplitude and phase stabilization of a laser under closed loop feedback to the power of the laser pump source.

The ultimate noise limit of a feedback loop is set by the vacuum noise introduced at the feedback beamsplitter and by the noise floor of the detection system. In the case of a frequency (or equivalently quadrature phase noise) stabilization scheme, this noise floor is typically far below the Schawlow-Townes limit for a free-running laser. In the case of an intensity stabilization scheme, this noise floor approaches the quantum noise limit, QNL.

In the case where the feedback loop acts on the amplitude noise of the laser and drives the amplitude noise to the theoretical minimum set by the beamsplitter, the phase noise is also reduced to a level that approaches the Schawlow-Townes limit. In the case where the feedback loop acts on the phase noise of the laser and drives the phase noise to the theoretical minimum set by the beamsplitter, the amplitude noise can approach or even fall below the quantum noise limit. At higher frequencies where the dominant noise feature is the resonant relaxation oscillation, and pump noise is only one contributor to the noise spectrum, the noise cannot be suppressed by a current locking scheme alone.

ACKNOWLEDGMENTS

This work was supported in part by the Australian Research Council and by Grant No. SFB407 of the Deutsche Forschungsgemeinschaft.

[1] B. Willke and the GEO600-Team, Class. Quantum Grav. **21**, 417 (2004).
[2] B. Abbott and the LIGO Science Collaboration, Nucl. Instrum. Methods Phys. Res. A **517**, 154 (2004).
[3] F. Acernese and the VIRGO collaboration, Class. Quantum Grav. **21**, 385 (2004).
[4] M. Ando and the TAMA collaboration, Class. Quantum Grav. **19**, 1409 (2002).
[5] H. A. Bachor and T. C. Ralph, *A Guide to Experiments in Quantum Optics*, 2nd ed. (Wiley-VCH, Wenheim, 2003).
[6] T. J. Kane and R. L. Byer, Opt. Lett. **10**, 65 (1985).
[7] T. C. Ralph, C. C. Harb, and H.-A. Bachor, Phys. Rev. A **54**, 4359 (1996); T. C. Ralph, *ibid.* **55**, 2326 (1997).
[8] H. A. Haus and Y. Yamamoto, Phys. Rev. A **34**, 270 (1986).
[9] H. M. Wiseman, G. M. Taubman, and H.-A. Bachor, Phys. Rev. A **51**, 3227 (1995).
[10] B. C. Buchler, E. H. Huntington, C. C. Harb, and T. C. Ralph, Phys. Rev. A **57**, 1286 (1998).
[11] B. Willke, O. S. Brozek, K. Danzmann, V. Quetschke, and S. Gossler, Opt. Lett. **25**, 1019 (2000).
[12] M. Heurs, V. M. Quetschke, B. Willke, K. Danzmann, and I. Freitag, Opt. Lett. **29**, 2148 (2004).
[13] M. Heurs, T. Meier, V. M. Quetschke, B. Willke, I. Freitag, and K. Danzmann, Appl. Phys. B: Lasers Opt. **85**, 79 (2006); M. Heurs, Ph.D. thesis, University of Hannover, 2004.
[14] R. W. P. Drever, J. L. Hall, F. V. Kowalski, J. Hough, G. M. Ford, A. J. Munley, and H. Ward, Appl. Phys. B: Photophys. Laser Chem. **31**, 97 (1983).
[15] C. C. Harb *et al.*, J. Opt. Soc. Am. B **14**, 2936 (1997).
[16] E. H. Huntington, T. C. Ralph, and I. Zawischa, J. Opt. Soc. Am. B **17**, 280 (2000).
[17] F. W. Quelle, Jr., Appl. Opt. **5**, 633 (1966).
[18] W. Koechner, *Solid-State Laser Engineering*, 4th ed. (Springer, Berlin, 1996).
[19] S. C. Tidwell, J. F. Seamans, M. S. Bowers, and A. K. Cousins, IEEE J. Quantum Electron. **28**, 997 (1992).
[20] T. Y. Fan, IEEE J. Quantum Electron. **29**, 1457 (1993).
[21] M. Cerdonio, L. Conti, A. Heidmann, and M. Pinard, Phys. Rev. D **63**, 082003 (2001).
[22] M. De Rosa, L. Conti, M. Cerdonio, M. Pinard, and F. Marin, Phys. Rev. Lett. **89**, 237402 (2002).
[23] D. F. Walls and G. J. Milburn, *Quantum Optics* (Springer-Verlag, New York, 1994).
[24] Y.-J. Cheng, IEEE J. Quantum Electron. **30**, 1498 (1994).
[25] A. E. Siegman, *Lasers* (University Science, Mill Valley, CA, 1986).
[26] E. H. Huntington and T. C. Ralph, J. Opt. B: Quantum Semiclassical Opt. **4**, 123 (2002).
[27] M. Tinto, D. A. Shaddock, J. Sylvestre, and J. W. Armstrong, Phys. Rev. D **67**, 122003 (2003).